Solar Brightness Temperature and Corresponding Antenna Noise Temperature at Microwave Frequencies

Christian Ho,* Stephen Slobin,† Anil Kantak,* and Sami Asmar*

In this study, the fluctuation ranges and mean values of solar brightness temperatures at microwave frequencies are estimated using solar radio emission fluxes at 2800 and 8800 MHz measured through several solar cycles. These variations include both short-term (daily) and long-term (11-year solar cycle) changes. The corresponding antenna noise temperatures at S-, X-, and Ka-bands are calculated for various antenna beamwidths and pointing offsets. The results are applied to the link design for a Lagrangian-orbit mission with a low-gain antenna at S-band.

I. Introduction

The solar radiation spectrum covers all frequencies ranging from radio to optical (infrared, visible, and ultraviolet). The solar radiance and temperature are a function of the wavelength. In the optical range (100-nm to 1000-nm wavelength), the Sun can be treated as a blackbody with a constant temperature of about 6000 K. The radiation flux is quite stable, with very small changes over the solar cycle. However, in the radio frequency band (1 cm to 30 cm wavelength, approximately), the radiance for a disturbed Sun is significantly different from that for a quiet Sun [1,2,3].

As shown in Figure 1, the solar flux density is equal to that from a blackbody radiator at 6000 K at wavelengths less than about 1.0 cm (a frequency greater than about 30 GHz), but the spectral density becomes much greater at longer wavelengths for both a quiet and disturbed Sun. An active Sun has much larger flux density than does a quiet Sun in the frequency range between 100 MHz (3-m wavelength) and 30 GHz (1 cm wavelength). These elevated fluxes come mainly from the contribution of the solar corona and the chromosphere, a thin layer just above the visible photosphere [1,2].

For the design of a telecommunications link between a spacecraft and the Deep Space Network (DSN), we are concerned with the system noise temperature at microwave frequencies during solar conjunction when the line of sight to the spacecraft is near the Sun, or for Lagrangian-orbit missions when the ground receiving antenna also points near the Sun.

* Communication Architectures and Research Section.
† Communications Ground Systems Section.

The research described in this publication was carried out by the Jet Propulsion Laboratory, California Institute of Technology, under a contract with the National Aeronautics and Space Administration. Government sponsorship acknowledged.

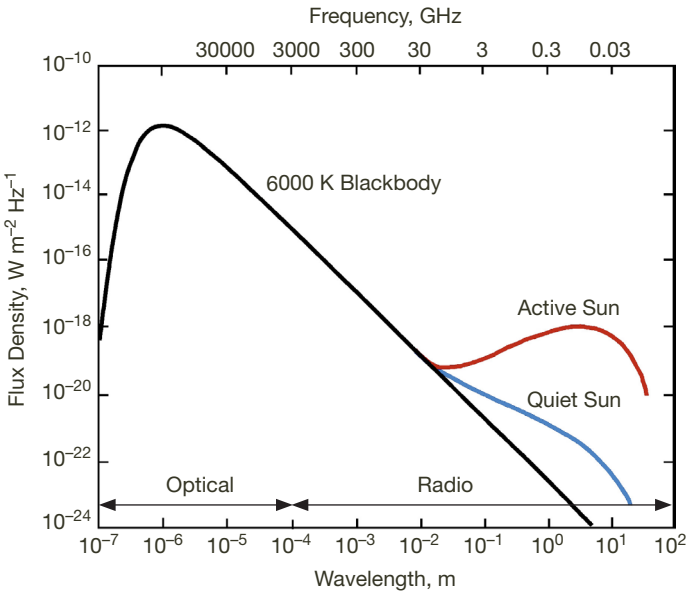

Figure 1. The solar radiation spectrum at optical and radio frequencies. At wavelengths greater than 1 cm, the radiance from an active Sun is much larger than from a quiet Sun and from a blackbody at 6000 K (figure after [1,2]).

Even though many theoretical and experimental studies have been done in defining the solar brightness temperatures and power fluxes [1,2,3,4], in the microwave frequency range (especially in DSN communication bands), the solar cycle variations of the brightness temperature and its fluctuation range have not been specifically determined. The fluctuation range of the antenna noise temperature and, consequently, fluctuation range of the link margins are not known.

This study uses measurements of solar flux made at 10.7-cm wavelength (2800 MHz) and at 3.4-cm wavelength (8800 MHz) through several solar cycles to infer the solar brightness temperature at 2.3 GHz (S-band), 8.5 GHz (X-band), and 32 GHz (Ka-band), and to examine their solar cycle dependence, their mean values, and their fluctuation ranges. As a final result, the corresponding antenna noise temperatures at microwave frequencies and telecommunication link margins are defined.

II. Solar Radiation Fluxes and Brightness Temperatures at Microwave Frequencies

A. Solar Power Flux and Sunspot Numbers

In the radio frequency range, the radiant power fluxes for a disturbed Sun have both slowly varying and rapidly varying components. The fluxes at different wavelengths come from different regions of the Sun. The millimeter-wavelength flux is radiated from the visible photosphere, while longer wavelengths originate from the higher (outer) regions of the Sun (e.g., the corona) [1].

There are two types of solar flux variations: long-term and short-term. The long-term variations include annual and 11-year solar cycle variations, while short-term variations usually mean changes within days. Measurements show that the solar flux at 10.7-cm wavelength (2800 MHz) can change by a factor of 4 (from 70 SFU to 280 SFU) through the solar cycle [5,6], where one solar flux unit (SFU) is 10^{-22} W m^{-2} Hz^{-1}.

Variations of sunspot number and radio emission at 10.7 cm over 58 years (six solar cycles) are shown in Figure 2. During solar maximum years, the Sun becomes very active. Sunspot numbers increase by a factor of 10 relative to the number at solar minimum, and the disturbed areas on the photosphere become larger. Increased emission at microwave frequencies is strongly related to the active Sun. As shown in Figure 2, the slowly varying components of solar radio emission have high correlation with the sunspot numbers. The emission measurements show that the rapidly varying components (such as daily variations) of solar flux also have larger variations during the solar maximum, but the correlation is not as strong as with the slow variations [5].

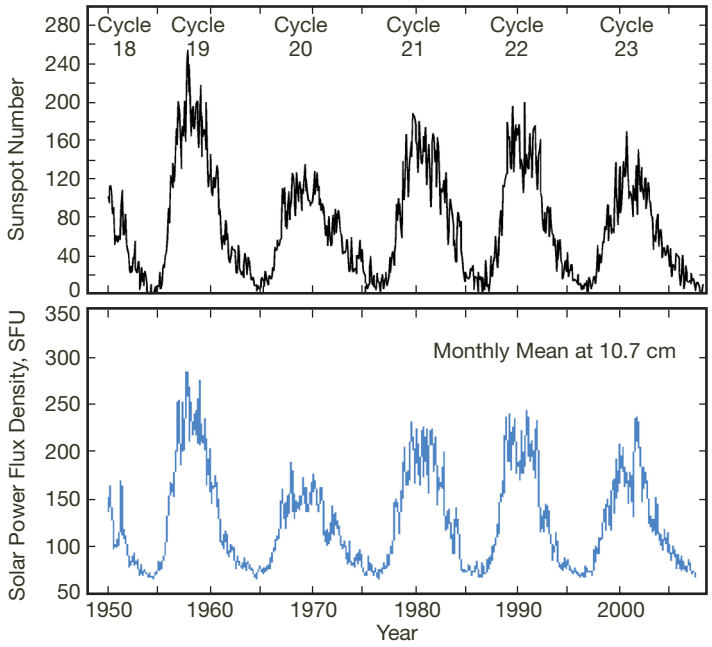

Figure 2. Long-term variations of sunspot numbers (top panel) and power flux density at 10.7 cm wavelength (bottom panel) through 58 years. Both data are plotted using monthly average measurements. It is obvious that the solar radiation at this wavelength has a very good correlation with sunspot numbers (data from [5,6]).

B. Solar Brightness Temperature at Microwave Frequencies

The solar brightness temperature for a quiet Sun observed during the solar minimum period can be different from that observed during other phases. There may be a factor of 4 to 10 variation at lower microwave frequencies (1 to 3 GHz).

The theoretical brightness temperature for a quiet Sun is shown in Figure 3 (curve A). To get this curve, it is assumed that there is a 10^6 K corona and a 30,000 K chromosphere [1,7,8].

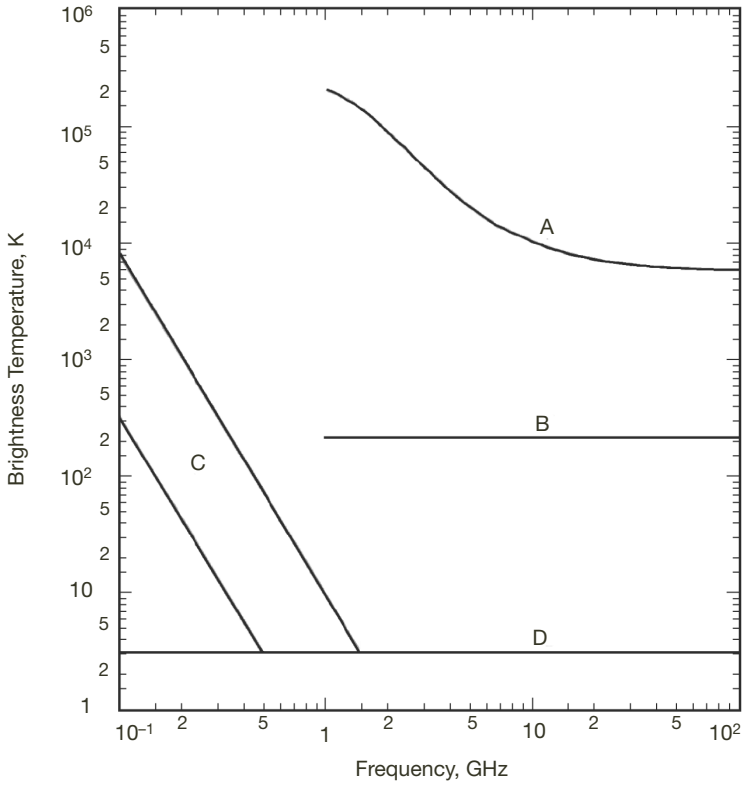

Figure 3. All noises from extraterrestrial sources. Line A is from a quiet Sun, while line B is from the Moon (all with 0.5-deg beamwidth diameter). Galactic noise (C, maximum to minimum) and cosmic background (D) are also shown. Lunar emission is independent of the frequency (figure after [7]).

It is seen that the brightness temperature decreases from 2×10^5 K at 1 GHz to 6000 K at 100 GHz.

The solar brightness temperature can be calculated from its radio emissions measured at 10.7 cm (2800 MHz) and 3.4 cm (8800 MHz) wavelength. Based on the Rayleigh-Jeans approximation for blackbody radiation at radio frequencies, the radio emission received in a given frequency band per unit effective area is defined as the power flux density, F_s, which is an integration of the radiance per unit bandwidth, B_λ, over a solid angle subtended by the source. The solar flux density is given by

$$F_s = B_\lambda \Omega_s = 2k_B T_d \Omega_s \lambda^{-2} \tag{1}$$

where F_s = power flux density, W m^{-2} Hz^{-1}
B_λ = spectral radiance, W m^{-2} Hz^{-1} sr^{-1}
Ω_s = solid angle, sr
k_B = Boltzmann's constant, J K^{-1}
T_d = brightness temperature, K
λ = wavelength, m

Converting the solid angle into degrees, when the angle is very small, the flux density can be approximately expressed as

$$F_s = 2k_B T_d \pi(\alpha\pi/180)^2 \lambda^{-2} \tag{2}$$

where α is the angular radius of the Sun in degrees (α = 0.25 deg).

Using the above equation and measured power flux density at 10.7 cm as shown in Figure 2, the Sun's brightness temperature can be calculated at 2800 MHz. For a flux density of 150 SFU (approximately the average value), the brightness temperature is 100,000 K. A periodic function is used to model the average trends of 10.7 cm measurements shown in Figure 2. Then, using this function, the solar brightness temperatures are generated for four solar cycles (from 1975 to 2015) as shown in Figure 4. This model will give a general range of daily and annual variations of the brightness temperature.

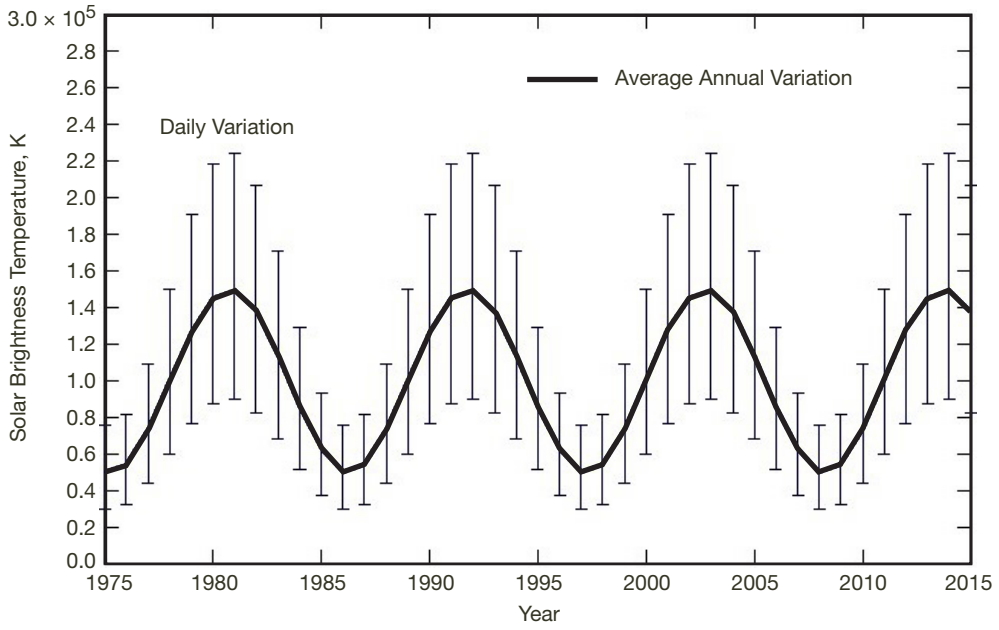

Figure 4. Solar cycle variation of the Sun's brightness temperature derived from radio emission (at 10.7 cm, 2800 MHz) measurements based on Figure 2. Both daily and annual variations are shown.

The emission measurements at 10.7 cm show that the daily variations (not shown in Figure 2) can have the same magnitude as does the annual variation. When the annual changes in the brightness temperature are about 10^5 K from the maximum to the minimum, there is a ~ $\pm 7 \times 10^4$ K daily change, which is superimposed on top of the annual changes at the solar maximum. From Figure 4, it is seen that over the solar cycle the average temperature has a value of 100,000 K, with a yearly average maximum of 150,000 K, and a yearly average minimum of 50,000 K.

Measurements show that the power flux density at 8.8 GHz (3.4 cm) is higher than that at 2.8 GHz (10.7 cm) by a factor of about 2.17 on average. As a result, the brightness temperature at 8.8 GHz is about 22 percent that at 2.8 GHz because of the smaller wavelength. Figure 5 shows the brightness temperature at 8.8 GHz based on the radio emission measurements at that frequency. Over the solar cycle, the average yearly value is 22,000 K, with yearly average maximum and minimum of 30,000 K and 14,000 K, respectively. It is seen that at higher frequency bands the daily fluctuations relative to their annual variations also become smaller.

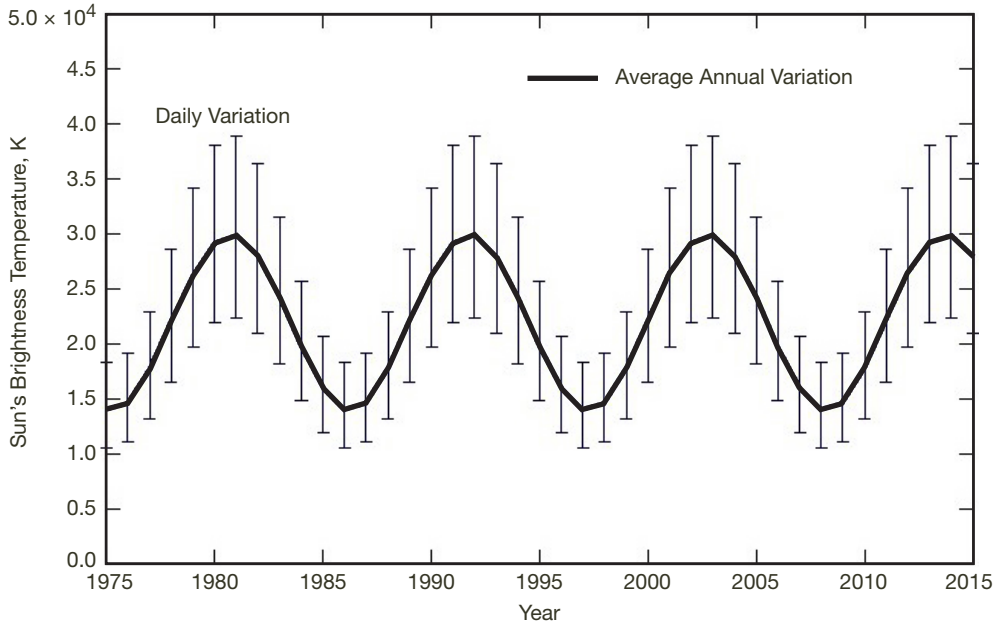

Figure 5. Solar cycle variation of the Sun's brightness temperature derived from radio emission measurements at 3.4 cm (8800 MHz). Both daily and annual variations are shown.

From the expressions given in [3], the brightness temperatures of a quiet Sun can be calculated at 32 GHz (0.937 cm wavelength). The daily and annual variations in the brightness temperature are shown in Figure 6. The average value is 10,000 K, and the maximum and minimum year-average values are about 12,500 K and 7500 K, respectively. Recent solar experimental measurements at 32 GHz [9] are consistent with these values.

The quiet-Sun brightness temperatures at 2.3 GHz (S-band) and 8.5 GHz (X-band) can also be estimated using [3]. At S-band, the value is about 29,800 K, and at X-band the value is about 16,100 K. These quiet-Sun values are comparable to the minimum values shown in Figures 4 and 5, at somewhat different frequencies.

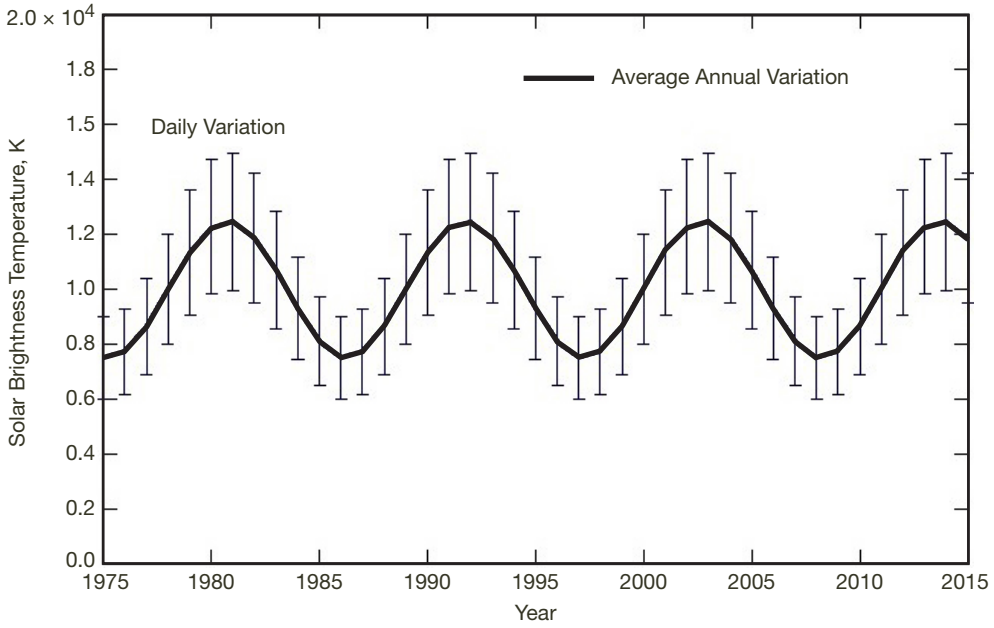

Figure 6. Solar cycle variation of the Sun's brightness temperature at 32 GHz (Ka-band). Both daily and annual variations are shown.

C. Antenna Noise Temperature When Pointing at the Sun

Using the Sun's brightness temperatures at radio frequencies, one can calculate the antenna noise temperature when it points at the Sun. When an antenna points at a blackbody, its noise temperature can be calculated as follows [10].[1]

The antenna noise temperature caused by blackbody radiation greatly depends on the beamwidth of the antenna and the relative location of its boresight axis to the blackbody disk. This geometry and all parameters used in this calculation are shown in Figure 7. In the figure, a receiving antenna's half-power beamwidth (HPBW) relative to a circular blackbody is shown. We model the antenna beams with two cases: HPBW << D_θ, and HPBW >> D_θ, where D_θ is the angular diameter of the blackbody disk. The blackbody's radius is r_d, while the distance between the beam center and disk center is l_d. The distance between the receiving antenna and the blackbody is not important for this scenario because angular distances are used.

In most blackbody cases, the brightness temperature is assumed constant over the entire surface of the body, and the blackbody radiates isotropically in all directions, i.e., the disk observed at radio frequencies has the same diameter as the optical disk and the temperature distribution across the disk is uniform. The antenna noise temperature increase normalized to the blackbody brightness temperature is then given as

$$\frac{T_{incr}}{T_b} = \frac{\int_{disk} G_r(\theta,\phi)\, T_b\, d\Omega}{\int_{4\pi} G_r(\theta,\phi)\, T_b\, d\Omega} \tag{3}$$

[1] A. V. Kantak and S. D. Slobin, *System Noise Temperature Increase from the Sun, Moon, or Planet Blackbody Disk Temperature*, JPL D-33697 (internal document), Jet Propulsion Laboratory, Pasadena, California, December 1, 2005.

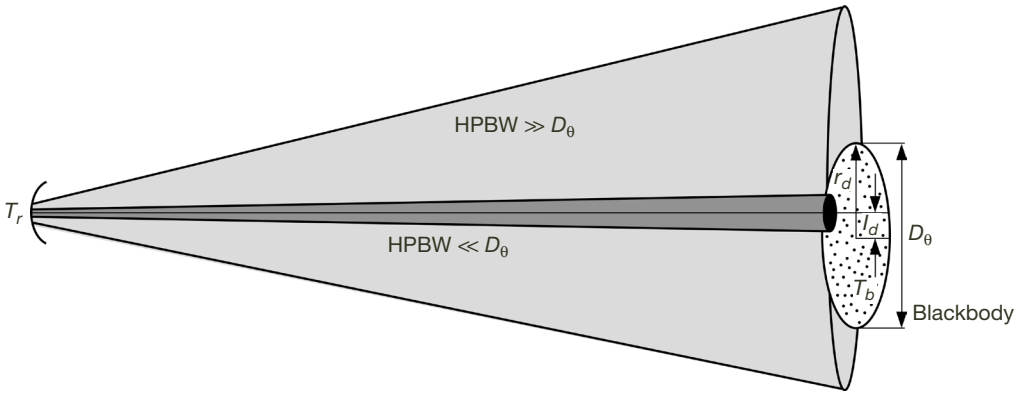

Figure 7. Geometry of antenna beams with two types of beamwidths relative to a blackbody [10].

where T_{incr} is the temperature increase, T_b is the blackbody brightness temperature, and $G_r(\theta,\phi)$ is the normalized power pattern of the receiving antenna when its boresight points at the blackbody. It should be understood that the integration in the numerator is over the solid angle of the blackbody disk only, and the integration in the denominator is over the entire space (4π).

The Bessel function approximation is used for the normalized power pattern (including mainlobe and sidelobes) of the antenna to compute the results:

$$G_{Bes}(\theta) = \left[\frac{2J_1\left(\frac{\pi D_a}{\lambda}\sin(\theta)\right)}{\frac{\pi D_a}{\lambda}\sin(\theta)}\right]^2 \tag{4}$$

where J_1 is the Bessel function of order 1, θ is the angle off antenna boresight, D_a is the antenna diameter, and λ is the associated wavelength. It should be noted that D_a and λ are in the same units. Substituting the above Bessel function approximation for the antenna gain pattern into the temperature increase equation and then integrating, the following results are obtained.

For a general case for various values of $HPBW \leq D_\theta$, the normalized antenna noise temperature increases are shown in Figure 8 as a function of antenna pointing offsets. The distance between the antenna beam center and the disk (blackbody) center has been normalized by the disk radius. We can see that for a high-gain antenna with a very narrow beam (such as a DSN 34-m antenna), when the beam is on the solar disk the antenna noise temperature (blue line) is almost the same as the blackbody brightness temperature, T_b. When the antenna beam points off the solar disk, the antenna temperature is reduced to below 5 percent of T_b.

The results presented above can be applied to a practical test case: James Webb Space Telescope (JWST) telecommunications link design. JWST has a Lagrangian (L2) orbit. The space-

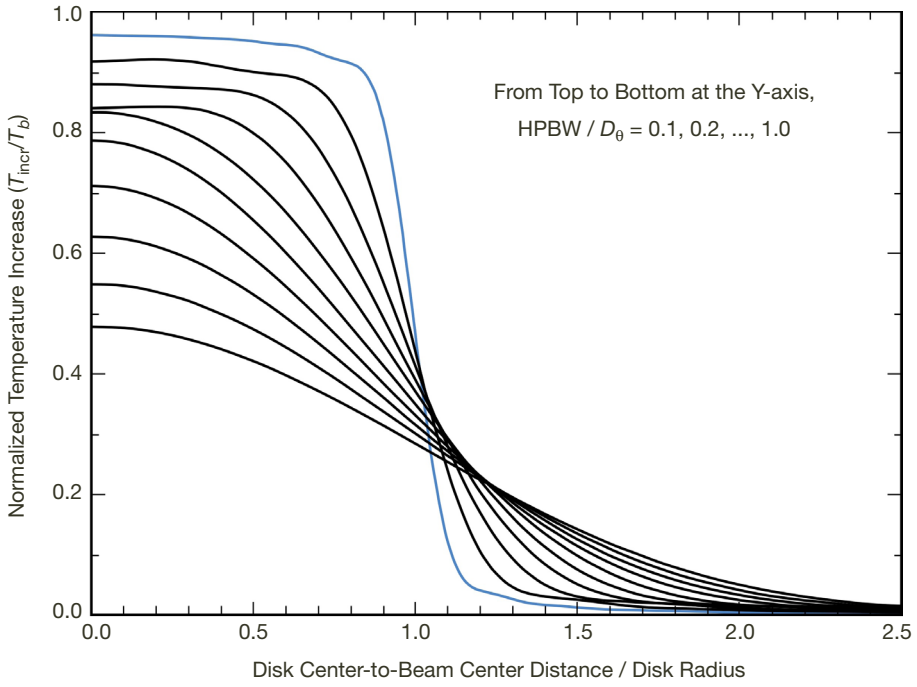

Figure 8. The normalized antenna noise temperature increase versus the normalized distance from the blackbody center when *HPBW* $\leq D_\theta$.

craft antenna has a 10-dB gain at 2.25 GHz. This is a low-gain, wide-beam antenna. When the spacecraft is receiving signals from Earth, its antenna is also pointing to the Sun at the same time. Based on the brightness temperature estimate at S-band, the antenna noise temperatures at various pointing offset angles can be calculated. The results of the system noise temperature and link margins are shown in Figure 9. From the figure, one can see that there are no significant differences in the link margins and temperature increases between 0 deg offset and 10 deg offset for this wide-beam antenna. For a 300,000 K solar noise temperature, the antenna noise temperature is about 24 K. The carrier margin is about 25 dB, while the data margin is about 9 dB. The antenna noise temperature increase is so low that pointing near the Sun will not cause a significant problem in this link design. However, this will not be the case for a high-gain antenna where the antenna beamwidth is comparable to or smaller than the solar disk, as shown in Figure 8.

III. Summary

In this study, a general range of solar brightness temperatures and the antenna noise temperatures at microwave frequencies have been defined using average solar cycle models. These estimates can be used by systems engineers for the design of telecommunication systems. Based on solar radio emissions measured at 2.8 and 8.8 GHz, the solar brightness temperatures have been derived, and a periodic model over the 11-year solar cycle has been presented. From the measured emission values at both frequencies, solar brightness temperatures have been developed for use at S-, X-, and Ka-bands. Solar cycle dependence of the

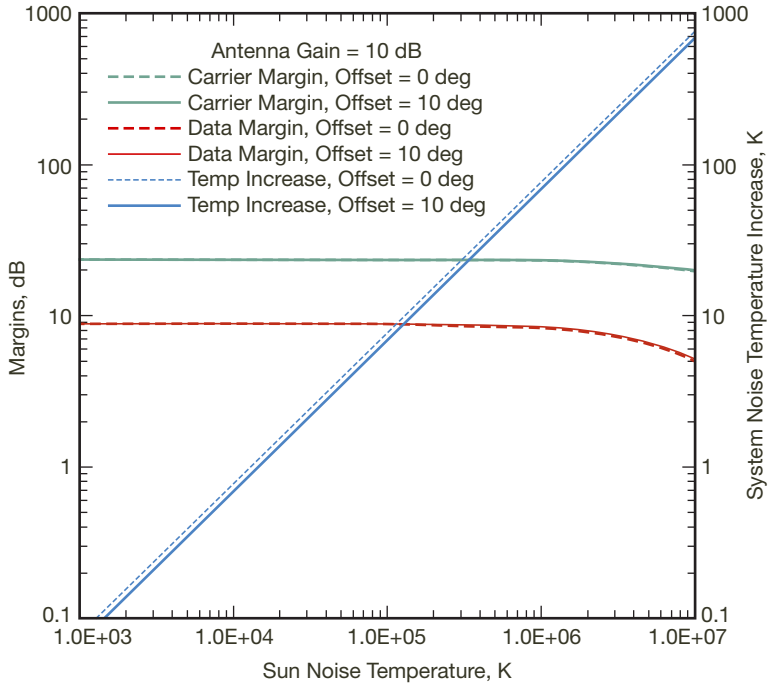

Figure 9. Antenna noise temperature and link margin as a function of the Sun's brightness temperature.

daily and annual variations of the brightness temperature is modeled. The average values and their minimum and maximum ranges are defined. An example is given for the JWST spacecraft S-band telecommunication link, which shows that for a very wide-beam antenna, pointing at or near the Sun has very little effect on the link margin.

Acknowledgment

The authors would like to thank Dr. Haiping Tsou for his review of this paper.

References

[1] S. L. Valley, *Handbook of Geophysics and Space Environments*, Air Force Cambridge Research Laboratories, Shea L. Valley, ed., New York: McGraw-Hill Book Company, Inc., 1965.

[2] J. D. Kraus, *Radio Astronomy*, 2nd ed., Powell, Ohio: Cygnus-Quasar Books, 1986.

[3] J. L. Linsky, "A Recalibration of the Quiet Sun Millimeter Spectrum Based on the Moon as an Absolute Radiometric Standard," *Solar Physics*, vol. 28, pp. 409–418, 1973.

[4] S. D. Slobin, T. Y. Otoshi, M. J. Britcliffe, L. S. Alvarez, S. R. Stewart, and M. M. Franco, "Efficiency Measurement Techniques for Calibration of a Prototype 34-Meter-Diameter Beam-Waveguide Antenna at 8.45 and 32 GHz," *IEEE Transactions on Microwave Theory and Techniques*, vol. 40, no. 6, pp. 1301–1309, June 1992.

[5] National Geophysical Data Center, Solar Data Services, Penticton/Ottawa 2800 MHz Solar Flux, 2007. http://www.ngdc.noaa.gov/stp/SOLAR/FLUX/flux.html

[6] National Geophysical Data Center, Solar Radio Fluxes, 2004. http://www.ngdc.noaa.gov/stp/SOLAR/ftpsolarradio.html

[7] "Radio Noise," ITU Recommendation, ITU-R P.372-8, International Telecommunication Union, Geneva, Switzerland, 2003.

[8] "Radio Emission from Natural Source in the Frequency Range above 50 MHz," Report 720-2, International Radio Consultative Committee (CCIR), International Telecommunication Union, Geneva, Switzerland, 1986.

[9] T. Y. Otoshi, "Measured Sun Noise Temperatures at 32 Gigahertz," *The Telecommunications and Mission Operations Progress Report*, vol. 42-145, Jet Propulsion Laboratory, Pasadena, California, pp. 1–32, May 15, 2001. http://ipnpr.jpl.nasa.gov/progress_report/42-145/145C.pdf

[10] C. Ho, A. Kantak, S. Slobin, and D. Morabito, "Link Analysis of a Telecommunication System on Earth, in Geostationary Orbit, and at the Moon: Atmospheric Attenuation and Noise Temperature Effects," *The Interplanetary Network Progress Report*, vol. 42-168, Jet Propulsion Laboratory, Pasadena, California, pp. 1–22, February 15, 2007. http://ipnpr.jpl.nasa.gov/progress_report/42-168/168E.pdf